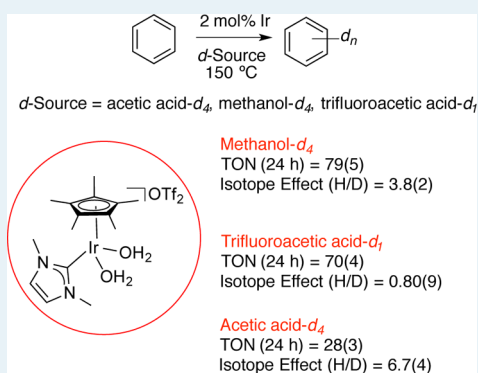


Effect of Solvent and Ancillary Ligands on the Catalytic H/D Exchange Reactivity of Cp\*Ir<sup>III</sup>(L) ComplexesMatthew C. Lehman,<sup>†</sup> J. Brannon Gary,<sup>‡</sup> Paul D. Boyle,<sup>†</sup> Melanie S. Sanford,<sup>‡</sup> and Elon A. Ison<sup>\*†</sup><sup>†</sup>Department of Chemistry, North Carolina State University, 2620 Yarbrough Drive, Raleigh, North Carolina 27695-8204, United States<sup>‡</sup>Department of Chemistry, University of Michigan, 930 North University Avenue, Ann Arbor, Michigan 48109, United States

## Supporting Information

**ABSTRACT:** The reactivity of a series of Cp\*Ir<sup>III</sup>(L) complexes that contain a diverse set of ancillary ligands, L (L = PMe<sub>3</sub>, N-heterocyclic carbene, NHC = 1,3-dimethylimidazol-2-ylidene, aqua, 4-*t*-butylpyridine, and 4-(2,4,6-tris-(4-*t*-butylphenyl)pyridinium)pyridine tetrafluoroborate) has been examined in catalytic H/D exchange reactions between C<sub>6</sub>H<sub>6</sub> and a series of deuterated solvents (methanol-*d*<sub>4</sub>, acetic acid-*d*<sub>4</sub>, and trifluoroacetic acid-*d*<sub>1</sub>). These studies demonstrate that (1) the mechanism of catalytic H/D exchange is significantly influenced by the nature of the solvent; (2) electron-donating ligands (PMe<sub>3</sub>, NHC) promote the formation of Ir hydrides in methanol-*d*<sub>4</sub>, and these are critical intermediates in catalytic H/D exchange processes; and (3) weak/poorly donating ligands (4-*t*-butylpyridine, 4-(2,4,6-tris-(4-*t*-butylphenyl)pyridinium)pyridine tetrafluoroborate and aqua) can support efficient H/D exchange catalysis in acetic acid-*d*<sub>4</sub>.

**KEYWORDS:** H/D exchange, C–H activation, C–H functionalization, Cp\*Ir<sup>III</sup> catalysts, kinetics, isotope effects



## INTRODUCTION

Iridium complexes have been shown to be highly effective for the stoichiometric activation of C–H bonds. In particular, extensive work by Bergman and co-workers has provided a detailed mechanistic picture of stoichiometric C–H activation reactions at Cp\*Ir(I) and Cp\*Ir(III) complexes.<sup>1</sup> Despite these pioneering studies, it has, until recently, remained challenging to exploit the facile C–H activation abilities of Cp\*Ir complexes in catalytic C–H functionalization reactions. In contrast, [Cp\*Rh] complexes have been shown to catalyze a wide variety of different ligand-directed C–H functionalization reactions.<sup>2</sup> For example, Glorius et al. recently demonstrated [Cp\*RhCl<sub>2</sub>]<sub>2</sub>-catalyzed C–H activation/halogenation sequences.<sup>2c</sup> To date, C–H functionalization of arenes and alkanes with the Cp\*Ir fragment remains underdeveloped.

Some of us have recently reported the Ir-catalyzed synthesis of benzochromenones from benzoic acids and alkynes.<sup>3</sup> In addition, Crabtree and co-workers have demonstrated the hydroxylation of C–H bonds catalyzed by a series of Cp\*Ir complexes.<sup>4</sup> The mechanisms for many of these transformations are still not established. Further, a detailed understanding of the factors that lead to efficient catalytic C–H functionalization with Cp\*Ir complexes is needed to rationally design new catalysts and catalytic transformations.

H/D exchange reactions between C<sub>6</sub>H<sub>6</sub> and deuterated solvents have been utilized recently to study C–H activation.<sup>5</sup> This method has the advantage that it does not depend on the isolation of transient organometallic complexes; furthermore, the reaction is believed to proceed via intermediates that are

directly relevant to catalytic C–H functionalization reactions. In this Article, we compare the reactivity of a series of Cp\*Ir<sup>III</sup>(L) complexes that contain a diverse set of ancillary ligands, L (L = PMe<sub>3</sub>, N-heterocyclic carbene, NHC = 1,3-dimethylimidazol-2-ylidene, aqua, 4-*t*-butylpyridine, and 4-(2,4,6-tris-(4-*t*-butylphenyl)pyridinium)pyridine tetrafluoroborate) in catalytic H/D exchange reactions between C<sub>6</sub>H<sub>6</sub> and a series of deuterated solvents (methanol-*d*<sub>4</sub>, acetic acid-*d*<sub>4</sub>, and trifluoroacetic acid-*d*<sub>1</sub>). These studies lead us to three key conclusions about C–H activation at Cp\*Ir complexes: (1) the mechanism of catalytic H/D exchange is significantly influenced by the nature of the solvent; (2) electron-donating ligands (PMe<sub>3</sub>, NHC) promote the formation of Ir hydrides in methanol-*d*<sub>4</sub>, and these species serve as intermediates in catalytic H/D exchange reactions; and (3) weak/poorly donating ligands (4-*t*-butylpyridine, 4-(2,4,6-tris-(4-*t*-butylphenyl)pyridinium)pyridine tetrafluoroborate and aqua)<sup>6</sup> can support efficient H/D exchange catalysis in acetic acid-*d*<sub>4</sub>. Overall, this work shows that by controlling the reaction conditions and the ancillary ligands coordinated to the metal, we can dramatically influence C–H activation reactivity. Since complexes featuring the Cp\*Ir(L) motif have been shown to be among the most effective in stoichiometric C–H activation reactions, the results presented here have significant potential

Received: June 3, 2013

Revised: August 24, 2013

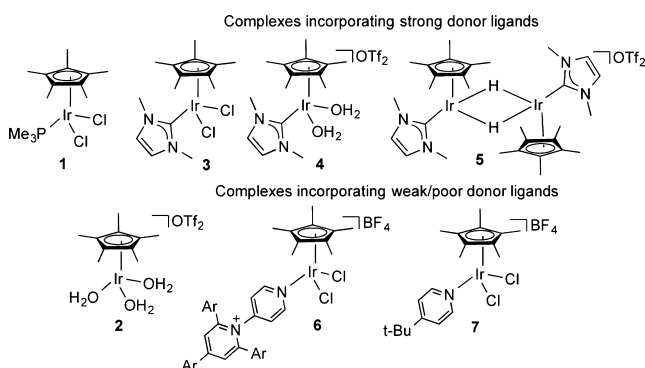
Published: August 27, 2013

implications for the development of C–H functionalization catalysts.

## RESULTS AND DISCUSSION

The Cp\*Ir<sup>III</sup>(L) complexes that were examined in the current study are depicted in Chart 1. The catalysts can be broadly

Chart 1. Catalysts Used in This Study



separated into two categories: (1) complexes incorporating strong donor ligands (PMe<sub>3</sub> and NHC) and (2) complexes incorporating weak donor ligands (H<sub>2</sub>O, pyridine derivatives). Notably, the diiridium hydride (**5**) was obtained by heating **4** in MeOH and was characterized by NMR spectroscopy and X-ray crystallography (Figure 1). The structure of **5** is similar to a

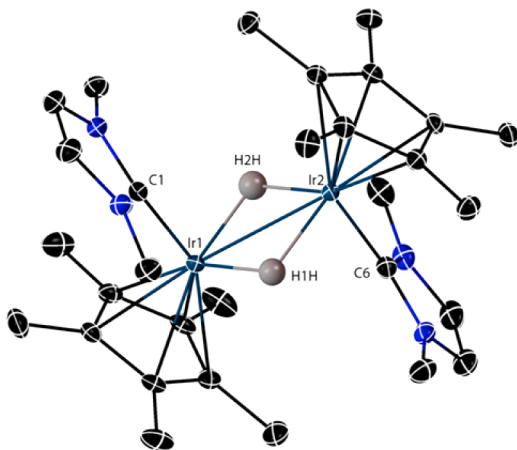


Figure 1. X-ray crystal structure of complex **5**. Ellipsoids are at the 50% probability level. Hydrogen atoms and triflate counterions were omitted for clarity. Selected bond lengths (Å): Ir1–Ir2, 2.7118(6); Ir1–C1, 2.0266(18); Ir2–C6, 2.0238(18).

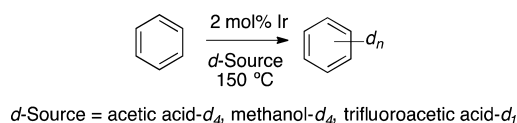
related complex reported by Yamaguchi and co-workers in which the tetramethyl-substituted NHC ligand was utilized (NHC = 1,3,4,5-tetramethylimidazol-2-ylidene).<sup>7</sup> The bond distance between the two Ir centers in **5** is 2.7118(6) Å. The geometry at each metal center is best described as a three-legged piano stool.

The syntheses of all of the catalysts utilized in this work are described in detail in the Supporting Information. Complexes **1–4** were previously examined as catalysts for H/D exchange reactions but have not been compared under the same conditions or studied mechanistically.<sup>8</sup> Further, although many of these complexes have been examined for H/D exchange, the mechanisms of these reactions have not been

systematically investigated. In particular, the role of solvents and ancillary ligands on catalytic H/D exchange reactivity has not been probed.

**H/D Exchange Reactions.** Deuterium incorporation into C<sub>6</sub>H<sub>6</sub> was examined for complexes **1–7**. A general reaction is shown in Scheme 1 with methanol-*d*<sub>4</sub>, acetic acid-*d*<sub>4</sub>, and

Scheme 1. Ir-Catalyzed H/D Exchange



trifluoroacetic acid-*d*<sub>1</sub> chosen as solvents and deuterium sources. Deuterium incorporation and turnover numbers (TONs) were determined by GC/MS utilizing a quantitative assay.<sup>5d</sup>

**Reactions in Methanol-*d*<sub>4</sub>.** The results of studies with methanol-*d*<sub>4</sub> are shown in Table 1. Catalyst **1**, when treated

Table 1. Results for Catalytic H/D Exchange Reactions with Complexes **1–7** in Methanol-*d*<sub>4</sub><sup>a</sup>

entry	catalyst	additive	TON <sup>b</sup>
1	<b>1</b>	none	11(3)
2	<b>1</b>	AgOTf <sup>c</sup>	179(3)
3	<b>2</b>	none	16.5(2)
4	<b>3</b>	none	9.3(4)
5	<b>3</b>	AgOTf <sup>c</sup>	44(9)
6	<b>4</b>	none	79(5)
7	<b>5</b>	none	76(6)
8	<b>6</b>	none	ND <sup>d</sup>
9	<b>6</b>	AgOTf <sup>c</sup>	3(0)
10	<b>7</b>	none	7(3)
11	<b>7</b>	AgOTf <sup>c</sup>	3(2)

<sup>a</sup>Reactions were run for 24 h with 25 equiv of deuterium source to C<sub>6</sub>H<sub>6</sub>. <sup>b</sup>Reported turnover numbers are the average of at least three trials and error is reported as the standard deviation of the mean. Turnover numbers (TONs) are calculated as moles of D incorporated per mole of catalyst. Conditions: benzene-*d*<sub>6</sub> (42 μL, 0.475 mmol), methanol-*d*<sub>4</sub> (11.9 mmol), and the respective iridium(III) catalyst (0.0095 mmol). <sup>c</sup>Two equivalents of AgOTf were added. <sup>d</sup>No deuterium incorporation was detected.

with AgOTf (entry 2), **4** (entry 6), and **5** (entry 7), showed the highest activity for H/D exchange. When **3** was treated with AgOTf (entry 5), the activity increased ~5-fold compared with the reaction of **3** without additive (entry 4). This suggests that AgOTf abstracts the chloride ligands in **3** to generate a more active catalyst. This effect is even more pronounced for **1**, as the TONs increase by more than an order of magnitude upon addition of AgOTf (entries 1 and 2). It is also important to note that in this solvent, H/D AgOTf does not catalyze exchange, and exchange does not take place without an Ir catalyst.

The TONs achieved with catalysts **4** and **5** (entries 6 and 7) are comparable. This is consistent with the observation that **5** is the major species in methanol when **4** is employed as the catalyst in H/D exchange reactions. Notably, complexes that contain moderate/weak donor ligands (H<sub>2</sub>O, **2**; pyridine, **6**; pyridinium, **7**) exhibit poor reactivity in methanol-*d*<sub>4</sub> (entries 3, 8–11).

Reactions in Trifluoroacetic Acid- $d_1$ . H/D exchange reactivity in trifluoroacetic acid- $d_1$  is shown in Table 2.

**Table 2. Results for Catalytic H/D Exchange Reactions with Complexes 1-7 in Trifluoroacetic Acid- $d_1$ <sup>a</sup>**

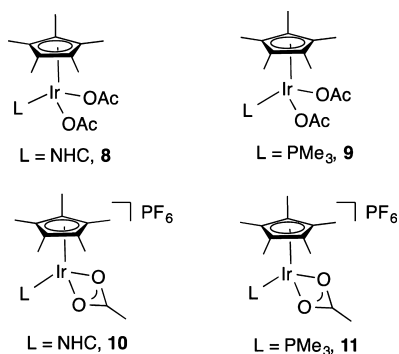
entry	catalyst	additive	TON <sup>b</sup>
1	1	none	159(2)
2	1	AgOTf <sup>c</sup>	146(2)
3	2	none	105(8)
4	3	none	18(2)
5	3	AgOTf <sup>c</sup>	51(1)
6	4	none	70(4)
7	6	none	7(3)
8	6	AgOTf <sup>c</sup>	95(5)
9	7	none	10(3)
10	7	AgOTf <sup>c</sup>	57(2)

<sup>a</sup>Reactions were run for 24 h with 25 equiv of deuterium source to  $C_6H_6$ . <sup>b</sup>Reported turnover numbers are the average of at least three trials, and error is reported as the standard deviation of the mean. Turnover numbers (TONs) are calculated as moles of D incorporated per mole of catalyst. Conditions: benzene- $d_6$  (42  $\mu$ L, 0.475 mmol), trifluoroacetic acid- $d_1$  (11.9 mmol), and the respective iridium(III) catalyst (0.0095 mmol). <sup>c</sup>Two equivalents of AgOTf were added.

Catalysts **1** ( $PMe_3$ ), **3** (NHC), and **4** (NHC) show similar TONs in trifluoroacetic acid- $d_1$  compared with the corresponding reaction in methanol- $d_4$ . In contrast, complex **2**, which contains weakly donating aqua ligands, exhibits poor activity in methanol- $d_4$  (TON = 16.5(2)) but improved reactivity in trifluoroacetic acid- $d_1$  (TON = 105(8), entry 3). Similarly, the pyridine- and pyridinium-containing catalysts **6** and **7**, when treated with AgOTf, exhibit improved reactivity in trifluoroacetic acid- $d_1$  (TON = 95(5) and 57(2), respectively) but poor activity in methanol- $d_4$  (TON = 3(0) and 3(2), respectively). It is also noteworthy that in trifluoroacetic acid- $d_1$ , there is significant H/D exchange when AgOTf is employed as a catalyst (44% deuterium incorporation after 24 h) and a small background reaction with the solvent in the absence of a metal (6% deuterium incorporation after 24 h). This is not the case in methanol- $d_4$  or acetic acid- $d_4$ .<sup>9</sup>

**Reactions in Acetic Acid- $d_4$ .** The data presented above show that the ancillary ligand (L) in the  $Cp^*Ir(L)$  fragment significantly affects the TONs for catalytic H/D exchange reactions in trifluoroacetic acid- $d_1$  and methanol- $d_4$ . In marked contrast, this is not the case in acetic acid- $d_4$ . Independently synthesized complexes **8–11** that incorporate acetate ligands in the primary coordination sphere are depicted in Chart 2. As

**Chart 2. Acetate-Containing Catalysts (8–11)**



shown in Figure 2, regardless of the ancillary ligands, all catalysts afforded approximately the same activity (TONs

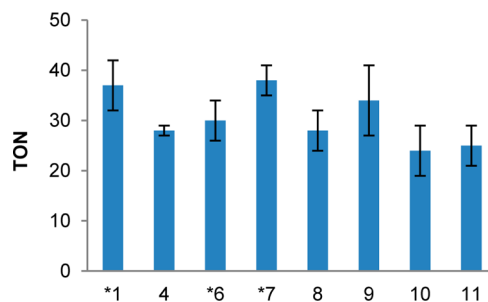


**Figure 2.** Catalytic H/D exchange reactions with complexes **1**, **4**, **6**, **7**, **8**, **9**, **10**, and **11** in acetic acid- $d_4$ . Conditions: Reactions were run for 24 h with 25 equiv of deuterium source to  $C_6H_6$ . The reported turnover numbers are the average of at least three trials, and error is reported as the standard deviation of the mean. An asterisk (\*) indicates that 2 equiv of AgOTf was added to the complex.

between 30 and 40), and complexes **8–11** performed as effectively as complexes **1**, **4**, **6**, and **7**.

**Mechanism for Catalytic H/D Exchange.** The H/D exchange data presented above suggests that different mechanisms for C–H activation may be operational when different solvents/deuterium sources are employed, as well as when the ancillary ligand L is varied. To investigate this possibility further, we examined the mechanism of the catalytic H/D exchange reaction with catalyst **4**. This catalyst was chosen because (1) its activity was among the highest of all the catalysts studied, (2) H/D exchange proceeded with this catalyst without the need for activation with AgOTf, and (3) high TONs were achieved with this catalyst in all three deuterium sources.

**Isotope Effects.** The effect of isotopic substitution on the catalytic H/D exchange reactions was first investigated. Isotope effects were determined by comparing the turnover numbers for deuterium exchange into  $C_6H_6$  (C–H activation) to turnover numbers for proton incorporation into  $C_6D_6$  (C–D activation).<sup>10</sup> Turnover numbers were obtained by GC/MS analysis of isotopologue concentrations. As shown in Table 3,

**Table 3. Isotope Effects for the Catalytic Deuterium Exchange into Benzene with a Variety of Solvents for Catalyst 4**

entry	solvent <sup>a</sup>	isotope effect <sup>b</sup>
1	methanol	3.8(2)
2	acetic acid	6.7(4)
3	trifluoroacetic acid	0.80(9)

<sup>a</sup>25 equiv of deuterium source to  $C_6H_6$ . <sup>b</sup>Reported isotope effects were determined by dividing the TON listed in Table 2 by the TON for the incorporation of protons into  $C_6D_6$ . All TONs were determined by GC/MS.

the isotope effect varies significantly as a function of the solvent/deuterium source. When the deuterium source/solvent is methanol- $d_4$  or acetic acid- $d_4$ , a primary isotope effect is observed (entries 1 and 2). In contrast, trifluoroacetic acid- $d_1$  affords an inverse isotope effect (entry 3). Similar isotope effects have been observed for other catalysts, and these data are presented in the Supporting Information.

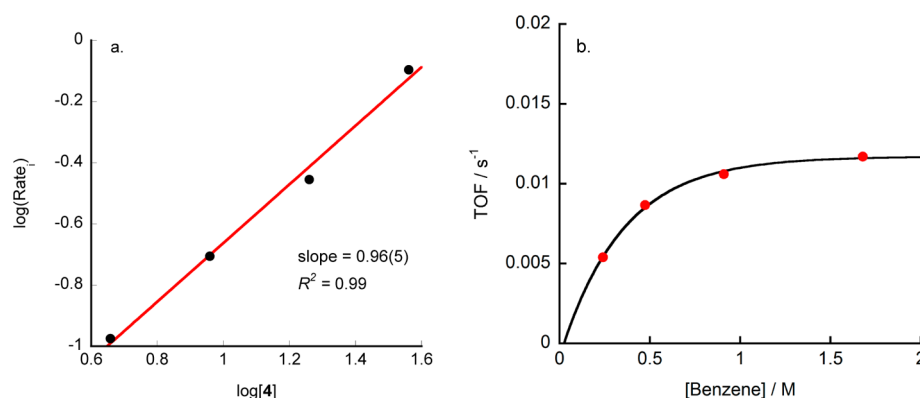
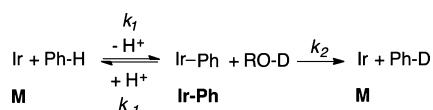


**Figure 3.** (a) Plot of initial rate of deuterium incorporation versus [4] in methanol- $d_4$ . (b) Plot of turnover frequency versus [benzene] in methanol- $d_4$ . Conditions: (a) Ir catalyst (0.0024, 0.0028, 0.0095, 0.019 mmol), benzene (0.475 mmol), methanol- $d_4$  (11.9 mmol) at 150 °C for 0.5 h. (b) Ir catalyst (0.0095 mmol), benzene (0.238, 0.475, 0.950, 1.68 mmol), methanol- $d_4$  (11.9 mmol) at 150 °C for 0.5 h. Data are fit with nonlinear least-squares fitting to an equation describing saturation in [benzene]:  $k_{\text{obs}} = k_2[\text{benzene}]/k' + [\text{benzene}]$  where  $k' = (k_{-1}[\text{H}^+] + k_2)/k_1$ . Turnover frequencies were determined by GC/MS.

**Mechanism of H/D Exchange in Methanol- $d_4$ .** The kinetics of the reaction catalyzed by 4 in  $\text{CD}_3\text{OD}$  was next examined in more detail. As shown in Figure 3, the reaction shows a first-order dependence on the Ir catalyst 4 (Figure 3a) and saturation kinetics in  $[\text{C}_6\text{H}_6]$  (Figure 3b).<sup>11</sup> A general mechanism that is consistent with the data is presented in Scheme 2 with the corresponding rate expression (assuming

**Scheme 2. Proposed Mechanism for the H/D Exchange Reaction of Benzene in Weakly and Moderately Acidic Solvents**



Michaelis Menten-type kinetics) depicted in eq 1. For this mechanism, benzene, **Ph-H**, is activated by a transition metal complex, **M**, to generate an Ir-phenyl complex, **Ir-Ph**. The **Ir-Ph** complex then reacts with the solvent, **ROD**, to form deuterated product, **Ph-D**, and regenerate the starting Ir complex, **M**.<sup>12</sup>

$$\text{rate} = \frac{k_1 k_2 [\text{Ph-H}][\text{M}]_{\text{T}}}{k_{-1}[\text{H}^+] + k_2 + k_1[\text{Ph-H}]} \quad (1)$$

**Mechanism of H/D Exchange in Trifluoroacetic Acid- $d_1$ .** A different mechanism appears to be operational in trifluoroacetic acid- $d_1$ . This hypothesis is based on the following experimental observations:

- (1) Catalytic H/D exchange reactivity for complexes with weak/poor donor ligands is enhanced in trifluoroacetic acid- $d_1$ .
- (2) Primary isotope effects are observed when the reactions are performed in methanol- $d_4$  and acetic acid- $d_4$ , whereas inverse isotope effects are observed in trifluoroacetic acid- $d_1$ .
- (3) Reactions performed in methanol- $d_4$  incorporate deuterium at a significantly faster rate than those performed in trifluoroacetic acid- $d_1$ . The reaction in methanol- $d_4$  showed an exponential appearance of the deuterated products and achieved the maximum turnovers in ~600 min (Supporting Information Figure S8).<sup>13</sup> In contrast,

the turnover numbers for the catalytic reaction performed in trifluoroacetic acid- $d_1$  increased at a significantly slower rate, and maximum turnovers were not achieved even after 4 d (Supporting Information). The reaction without a catalyst progressed at an even slower rate, and again, maximum turnovers were not reached after 4 d. These results clearly demonstrate that H/D exchange proceeds in trifluoroacetic acid- $d_1$  without the need for a catalyst; however, the rate of H/D exchange appears to be enhanced in the presence of 4.

In trifluoroacetic acid- $d_1$ , the order with respect to the concentration of 4 was 0.49(4) (Figure 4),<sup>14</sup> and the order with respect to the concentration of benzene was 0.88(9) (Figure 5).

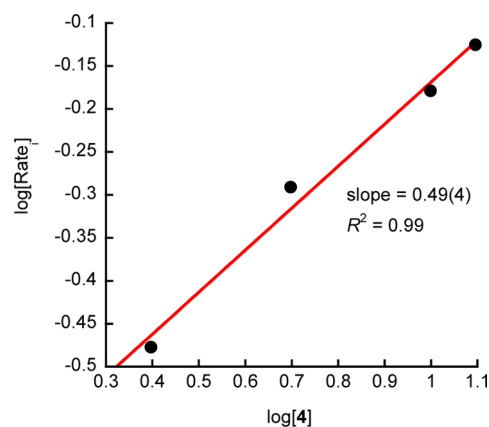


**Figure 4.** Plot of initial rate of deuterium incorporation versus [4] in trifluoroacetic acid- $d_1$ .

A proposed mechanism for H/D exchange in trifluoroacetic acid- $d_1$  that is consistent with all of this data is depicted in Scheme 3. Interaction of the solvent with the transition metal center results in the species **M(TFA)** and  $\text{D}^+$ . In a second step,  $\text{D}^+$  interacts with benzene by an electrophilic aromatic substitution ( $\text{Ar-S}_{\text{E}}$ ) mechanism with rate-determining formation of an arenium cation, followed by loss of  $\text{H}^+$  and the formation of the deuterated product. According to this mechanism, the role of the transition metal is to increase the Brønsted acidity of the solvent.



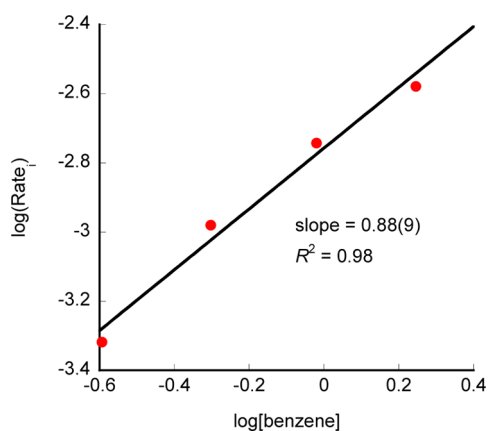
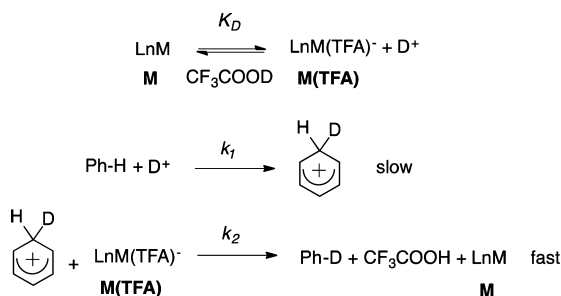


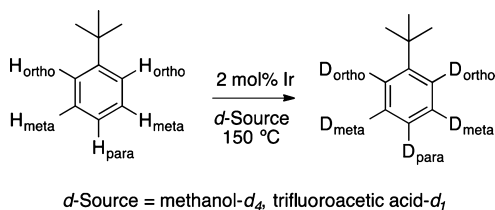
**Figure 5.** Plot of initial rate of deuterium incorporation versus [benzene] in trifluoroacetic acid- $d_1$ .

### Scheme 3. Proposed Mechanism for H/D Exchange in $\text{CF}_3\text{CO}_2\text{D}$



To further test the plausibility of an Ar- $S_E$  mechanism, we examined the site-selectivity of D incorporation into *t*-butyl benzene via  $^1\text{H}$  NMR spectroscopy (Scheme 4). If the H/D

### Scheme 4. Ir-Catalyzed H/D Exchange in *tert*-Butylbenzene



exchange reaction proceeds by an Ar- $S_E$  mechanism, then preferential deuterium incorporation at the ortho and para carbons should be observed because the *t*-butyl group is an ortho and para director.

As shown in Table 4, when the reaction was performed in trifluoroacetic acid- $d_1$  in the absence of a catalyst (entry 1), the

**Table 4. Site-Selectivity of Deuterium Incorporation (%) into the Ortho, Meta, and Para Positions of *t*-Butyl Benzene**

entry	catalyst	solvent	selectivity <sup>a</sup> (ortho/meta/para)
1	N/A	$\text{CF}_3\text{CO}_2\text{D}$	2.0/1.0/2.3
2	4	$\text{CF}_3\text{CO}_2\text{D}$	2.3/1.0/2.8
3	4	$\text{CD}_3\text{OD}$	0.42/1.0/0.42

<sup>a</sup>Deuterium incorporation (%) was determined by  $^1\text{H}$  NMR spectroscopy with a 0.1 M DSS internal standard in  $\text{D}_2\text{O}$  (DSS = sodium 4,4-dimethyl-4-silapentane-1-sulfonate)

site selectivity for deuterium incorporation into the ortho and para positions of *t*-butyl benzene was consistent with an Ar- $S_E$  mechanism. When the reaction was performed with catalyst 4, comparable site selectivity was observed (entry 2). In contrast, when the reaction was performed with 4 in methanol- $d_4$ , preferential deuterium incorporation into the meta position was observed.<sup>15</sup>

**d. Mechanism of H/D Exchange in Acetic Acid- $d_4$ .** As discussed above, when acetic acid- $d_4$  was used as a solvent, TONs for the various catalysts were essentially the same, regardless of the ancillary ligand. We hypothesize that this is because, in all cases, the catalytically active species has incorporated an acetate ligand from the acetic acid solvent. Importantly, the mechanism for C–H activation with complexes incorporating acetate ligands has been extensively studied.<sup>2q,u,16</sup> In many of these cases, the rate-determining step for C–H activation is not C–H bond cleavage, but binding of the substrate to the metal complex.<sup>17</sup> This is because the acetate ligand has a strong propensity to coordinate to the metal center in a bidentate fashion. Thus, C–H activation reactivity in these systems represents a subtle balance between (i) the equilibrium constant for  $\kappa^2$ -to- $\kappa^1$  isomerization of the acetate ligand (which opens a site at the metal for C–H  $\sigma$ -complex formation) and (ii) the ability of the carbonyl oxygen to deprotonate the coordinated C–H bond. We propose that these acetate ligand effects are the predominant factor that affects catalyst activity in acetic acid- $d_4$ , and thus, the ancillary ligand, L, has minimal influence on extent of H/D exchange. This proposal is supported by the H/D exchange reactivity described above (Figure 2) for Ir(III) acetate complexes 8–11 (Chart 2).<sup>18</sup> Significantly, catalysts 8–11 provided results nearly identical to catalysts 1, 4, 6, and 7 with TONs between 30 and 40.<sup>19</sup>

## CONCLUSIONS

In summary, this study has important implications for the design of  $\text{Cp}^*\text{Ir}^{\text{III}}(\text{L})$  complexes for C–H activation/functionalization. First, the solvent dramatically influences the mechanism of H/D exchange. We believe that organometallic mechanisms are occurring in acetic acid- $d_4$  and methanol- $d_4$ , whereas an Ar- $S_E$  mechanism is operating in trifluoroacetic acid- $d_1$ . The evidence supporting these proposals is the following:

- Primary isotope effects are observed in methanol- $d_4$  and acetic acid- $d_4$ , whereas inverse isotope effects are observed in trifluoroacetic acid- $d_1$  (Table 3).
- The rate of incorporation of deuterium is faster in methanol- $d_4$  than in trifluoroacetic- $d_1$ . H/D exchange in methanol- $d_4$  resulted in maximum turnovers after  $\sim 600$  min ( $k_{\text{obs}} = 1.7(5) \times 10^{-3} \text{ min}^{-1}$ ). In contrast, deuterium incorporation for the H/D exchange reaction in trifluoroacetic acid- $d_1$  did not achieve maximum turnovers, even after 4 d ( $k_{\text{obs}} = 3.3(7) \times 10^{-4} \text{ min}^{-1}$ ). Furthermore, reactions performed without a catalyst displayed a similar time profile ( $k_{\text{obs}} = 1.7(5) \times 10^{-4} \text{ min}^{-1}$ ).

Second, the ancillary ligand, L, also influences H/D exchange reactivity. The most active catalysts in methanol- $d_4$  contain strong donor ligands ( $\text{PMe}_3$  and NHC). For complexes with this class of ligand, hydride species have been identified in catalytic H/D exchange reactions in this solvent. In contrast, for complexes with moderate to weak donor ligands (aqua,

pyridine, pyridinium), no evidence for the formation of hydrides was observed. This difference in reactivity may be due to the ability of the complex to form a hydride by  $\beta$ -hydride elimination from an Ir-methoxy intermediate.

In acetic acid- $d_4$ , the ancillary ligand, L, appears to have a minimal impact on H/D exchange reactivity, as TONs of 30–40 are observed regardless of the ligand. In this solvent, C–H activation is proposed to proceed by an acetate-assisted  $\sigma$  bond metathesis mechanism. As a result, we hypothesize that H/D exchange reactivity is influenced most significantly by the  $\kappa^2$ -to- $\kappa^1$  isomerization of the acetate ligand and the ability of the carbonyl oxygen to deprotonate the coordinated C–H bond.

The results presented herein suggest that the proper choice of solvent and ancillary ligand could result in the rational design of new C–H functionalization catalysts that incorporate the Cp\*Ir(L) motif. The observation that complexes with strong donor ligands result in the formation of Ir hydrides and that these species enable C–H activation in weakly acidic polar solvents, such as methanol- $d_4$ , is particularly intriguing and suggests that catalysts may be developed that take advantage of these propensities.

## EXPERIMENTAL SECTION

**General Considerations.** The complexes **1**, **2**, **3**, **9**, and **11** were prepared according to published procedures.<sup>18,20</sup> Other reagents were purchased from commercial sources and used as received. <sup>1</sup>H and <sup>13</sup>C NMR spectra were recorded on a Varian Mercury 400 MHz or a Varian Mercury 300 MHz spectrometer at room temperature. <sup>1</sup>H and <sup>13</sup>C NMR chemical shifts are listed in parts per million (ppm) and are referenced to residual protons or carbons of the deuterated solvents, respectively. Mass spectrometry was performed by the North Carolina State University Mass Spectroscopy Facility using an Agilent Technologies 6210LC-TOF mass spectrometer (GC/MS). Elemental analyses were performed by Atlantic Microlabs, Inc. X-ray crystallography was performed at the X-ray Structural Facility of North Carolina State University by Dr. Paul Boyle.

**H/D Exchange Reactions.** Benzene (42  $\mu$ L, 0.475 mmol), deuterated solvent (11.9 mmol), and the respective iridium(III) catalyst (0.0095 mmol) were added to a  $\sim$ 3 mL Teflon sealed storage tube. The Schlenk tube was placed in a temperature-controlled oil bath set to 150  $^{\circ}$ C for 24 h. The reaction mixture was then cooled to room temperature and filtered through Celite. Reactions in acidic solvents were quenched with sodium bicarbonate and filtered through Celite. The resulting solution was then analyzed by GC/MS.

**Isotope Effect Studies.** Benzene- $d_6$  (42  $\mu$ L, 0.475 mmol), solvent (11.9 mmol), and the respective iridium(III) catalyst (0.0095 mmol) were added to a  $\sim$ 3 mL Teflon sealed storage tube. The Schlenk tube was placed in a temperature-controlled oil bath set to 150  $^{\circ}$ C for 24 h. The reaction mixture was then cooled to room temperature and filtered through Celite. Reactions in acidic solvents were quenched with sodium bicarbonate and filtered through Celite. The resulting solution was then analyzed by GC/MS.

**Time Profile Studies.** Benzene (42  $\mu$ L, 0.475 mmol), solvent (11.9 mmol), and the respective iridium(III) catalyst (0.0095 mmol) were added to a  $\sim$ 3 mL Teflon sealed storage tube. The Schlenk tube was placed in a temperature-controlled oil bath set to 150  $^{\circ}$ C. Aliquots were removed from the reaction mixture after various time intervals and analyzed by GC/MS.

**Kinetic Studies in Methanol- $d_4$ .** Benzene (10.5  $\mu$ L, 0.119 mmol; 21  $\mu$ L, 0.238 mmol; 42  $\mu$ L, 0.475 mmol; 84  $\mu$ L, 0.950

mmol), methanol- $d_4$  (480  $\mu$ L, 11.9 mmol), and the respective iridium(III) catalyst (0.0095 mmol) were added to a  $\sim$ 3 mL Teflon sealed storage tube. The Schlenk tube was placed in a temperature-controlled oil bath set to 150  $^{\circ}$ C for 0.5 h. The reaction mixture was then cooled to room temperature and filtered through Celite. The resulting solution was then analyzed by GC/MS.

**Kinetic Studies in Acetic Acid- $d_4$ .** Benzene (21  $\mu$ L, 0.238 mmol; 42  $\mu$ L, 0.475 mmol; 63  $\mu$ L, 0.713 mmol; 84  $\mu$ L, 0.950 mmol), acetic acid- $d_4$  (680  $\mu$ L, 11.9 mmol), and the respective iridium(III) catalyst (0.0095 mmol) were added to a  $\sim$ 3 mL Teflon sealed storage tube. The Schlenk tube was placed in a temperature-controlled oil bath set to 150  $^{\circ}$ C for 0.5 h. The reaction mixture was then cooled to room temperature, quenched with sodium bicarbonate, and filtered through Celite. The resulting solution was then analyzed by GC/MS.

**Kinetic Studies in Trifluoroacetic Acid- $d_1$ .** Benzene (21  $\mu$ L, 0.238 mmol; 42  $\mu$ L, 0.475 mmol; 84  $\mu$ L, 0.950 mmol; 126  $\mu$ L, 1.43 mmol), trifluoroacetic acid- $d_1$  (680  $\mu$ L, 11.9 mmol), and the respective iridium(III) catalyst (0.0095 mmol) were added to a  $\sim$ 3 mL Teflon sealed storage tube. The Schlenk tube was placed in a temperature-controlled oil bath set to 150  $^{\circ}$ C for 0.5 h. The reaction mixture was then cooled to room temperature, quenched with sodium bicarbonate, and filtered through Celite. The resulting solution was then analyzed by GC/MS.

**Initial Rate of Deuterium Incorporation As a Function of [4] in Methanol- $d_4$ .** Benzene (42  $\mu$ L, 0.475 mmol), methanol- $d_4$  (480  $\mu$ L, 11.9 mmol), and **4** (1.8 mg, 0.0024 mmol; 3.6 mg, 0.0048 mmol; 7.2 mg, 0.0095 mmol; 14.4 mg, 0.019 mmol) were added to a  $\sim$ 3 mL Teflon sealed storage tube. The tube was placed in a temperature-controlled oil bath set to 150  $^{\circ}$ C for 15 min. The reaction was then cooled to room temperature and filtered through Celite. The resulting solution was then analyzed by GC/MS. Initial rate data were obtained by dividing the TONs obtained from the assay by time (15 min). A plot of log (initial rate)-versus-log [4] was linear ( $R^2 = 0.99$ ).

**Initial Rate of Deuterium Incorporation as a Function of [4] in Trifluoroacetic Acid- $d_1$ .** Benzene (42  $\mu$ L, 0.475 mmol), trifluoroacetic acid- $d_1$  (0.911  $\mu$ L, 11.9 mmol), and **4** (1.8 mg, 0.0024 mmol; 3.6 mg, 0.0048 mmol; 7.2 mg, 0.0095 mmol; 14.4 mg, 0.019 mmol) were added to a  $\sim$ 3 mL Teflon sealed storage tube. The tube was placed in a temperature-controlled oil bath set to 150  $^{\circ}$ C for 7 h. The reaction mixture was quenched with sodium bicarbonate and filtered through Celite. The resulting solution was analyzed by GC/MS. Initial rate data were obtained by dividing the TONs obtained from the assay by time (420 min). A plot of log (initial rate)-versus-log [4] was linear.

## ASSOCIATED CONTENT

### Supporting Information

Syntheses of complexes, spectra, kinetic data, X-ray experimental for **4**. This material is available free of charge via the Internet at <http://pubs.acs.org>.

## AUTHOR INFORMATION

### Corresponding Author

\*E-mail: [eaison@ncsu.edu](mailto:eaison@ncsu.edu).

### Notes

The authors declare no competing financial interests.

## ACKNOWLEDGMENTS

This work was supported by the NSF as part of the Center for Enabling New Technologies through Catalysis (CENTC), CHE-0650456, and CHE-1205189. We thank Karen I. Goldberg, D. Michael Heinekey, and William D. Jones for helpful discussions.

## REFERENCES

- (1) (a) Bergman, R. G. *Science* **1984**, *223*, 902–908. (b) Bergman, R. G. *Nature* **2007**, *446*, 391–393. (c) Janowicz, A. H.; Bergman, R. G. *J. Am. Chem. Soc.* **1982**, *104*, 352–354.
- (2) (a) Ueura, K.; Satoh, T.; Miura, M. *Org. Lett.* **2007**, *9*, 1407–1409. (b) Song, G.; Gong, X.; Li, X. *J. Org. Chem.* **2011**, *76*, 7583–7589. (c) Schroeder, N.; Wencel-Delord, J.; Glorius, F. *J. Am. Chem. Soc.* **2012**, *134*, 8298–8301. (d) Satoh, T.; Miura, M. *Chem.—Eur. J.* **2010**, *16*, 11212–11222. (e) Rakshit, S.; Grohmann, C.; Besset, T.; Glorius, F. *J. Am. Chem. Soc.* **2011**, *133*, 2350–2353. (f) Patureau, F. W.; Nimphius, C.; Glorius, F. *Org. Lett.* **2011**, *13*, 6346–6349. (g) Patureau, F. W.; Glorius, F. *J. Am. Chem. Soc.* **2010**, *132*, 9982–9983. (h) Patureau, F. W.; Besset, T.; Kuhl, N.; Glorius, F. *J. Am. Chem. Soc.* **2011**, *133*, 2154–2156. (i) Patureau, F. W.; Besset, T.; Glorius, F. *Angew. Chem., Int. Ed.* **2011**, *50*, 1064–1067. (j) Parthasarathy, K.; Cheng, C.-H. *J. Org. Chem.* **2009**, *74*, 9359–9364. (k) Park, S. H.; Kim, J. Y.; Chang, S. *Org. Lett.* **2011**, *13*, 2372–2375. (l) Park, J.; Park, E.; Kim, A.; Lee, Y.; Chi, K.-W.; Kwak, J. H.; Jung, Y. H.; Kim, I. S. *Org. Lett.* **2011**, *13*, 4390–4393. (m) Mochida, S.; Umeda, N.; Hirano, K.; Satoh, T.; Miura, M. *Chem. Lett.* **2010**, *39*, 744–746. (n) Mochida, S.; Hirano, K.; Satoh, T.; Miura, M. *J. Org. Chem.* **2011**, *76*, 3024–3033. (o) Li, Y.; Zhang, X.-S.; Chen, K.; He, K.-H.; Pan, F.; Li, B.-J.; Shi, Z.-J. *Org. Lett.* **2012**, *14*, 636–639. (p) Hyster, T. K.; Rovis, T. *Chem. Commun.* **2011**, *47*, 11846–11848. (q) Hyster, T. K.; Rovis, T. *J. Am. Chem. Soc.* **2010**, *132*, 10565–10569. (r) Guimond, N.; Gorelsky, S. I.; Fagnou, K. *J. Am. Chem. Soc.* **2011**, *133*, 6449–6457. (s) Grohmann, C.; Wang, H.; Glorius, F. *Org. Lett.* **2012**, *14*, 656–659. (t) Du, Y.; Hyster, T. K.; Rovis, T. *Chem. Commun.* **2011**, *47*, 12074–12076. (u) Colby, D. A.; Tsai, A. S.; Bergman, R. G.; Ellman, J. A. *Acc. Chem. Res.* **2012**, *45*, 814–825. (v) Gong, T.-J.; Xiao, B.; Liu, Z.-J.; Wan, J.; Xu, J.; Luo, D.-F.; Fu, Y.; Liu, L. *Org. Lett.* **2011**, *13*, 3235–3237. (w) Hartwig, J. F. *Acc. Chem. Res.* **2012**, *45*, 864–873 and references therein..
- (3) Engelman, K. L.; Feng, Y.; Ison, E. A. *Organometallics* **2011**, *30*, 4572–4577.
- (4) (a) Zhou, M.; Schley, N. D.; Crabtree, R. H. *J. Am. Chem. Soc.* **2010**, *132*, 12550–12551. (b) Zhou, M.; Balcells, D.; Parent, A. R.; Crabtree, R. H.; Eisenstein, O. *ACS Catal.* **2012**, *2*, 208–218. (c) Zhou, M.; Hintermair, U.; Hashiguchi, B. G.; Parent, A. R.; Hashmi, M. E.; Periana, R. A.; Brudwig, G. W.; Crabtree, R. H. *Organometallics* **2013**, *32*, 957–965. (d) Hintermair, U.; Sheehan, S. W.; Parent, A. R.; Ess, D. H.; Richens, D. T.; Vaccaro, P. H.; Brudwig, G. W.; Crabtree, R. H. *J. Am. Chem. Soc.* **2013**, *135*, 10837–10851.
- (5) (a) Emmert, M. H.; Cook, A. K.; Xie, Y. J.; Sanford, M. S. *Angew. Chem., Int. Ed. Engl.* **2011**, *50*, 9409–12. (b) Emmert, M. H.; Gary, J. B.; Villalobos, J. M.; Sanford, M. S. *Angew. Chem., Int. Ed.* **2010**, *49*, 5884–5886. (c) Hickman, A. J.; Cismesia, M. A.; Sanford, M. S. *Organometallics* **2012**, *31*, 1761–1766. (d) Hickman, A. J.; Villalobos, J. M.; Sanford, M. S. *Organometallics* **2009**, *28*, 5316–5322. (e) Young, K. J. H.; Meier, S. K.; Gonzales, J. M.; Oxgaard, J.; Goddard, W. A., III; Periana, R. A. *Organometallics* **2006**, *25*, 4734–4737.
- (6) Gary, J. B.; Cook, A. K.; Sanford, M. S. *ACS Catal.* **2013**, *3*, 700–703.
- (7) Hanasaka, F.; Fujita, K.-i.; Yamaguchi, R. *Organometallics* **2005**, *24*, 3422–3433.
- (8) (a) Corberan, R.; Sanau, M.; Peris, E. *J. Am. Chem. Soc.* **2006**, *128*, 3974–3979. (b) Cesar, V.; Gade, L. H.; Bellemin-Laponnaz, S. In *RSC Catalysis Series*; Diez-Gonzales, S., Ed.; Royal Society of Chemistry: London, 2011; Vol. 6, pp 228–251. (c) Hanasaka, F.; Fujita, K.-i.; Yamaguchi, R. *Organometallics* **2006**, *25*, 4643–4647. (d) Feng, Y.; Jiang, B.; Boyle, P. A.; Ison, E. A. *Organometallics* **2010**, *29*, 2857–2867. (e) Yung, C. M.; Skaddan, M. B.; Bergman, R. G. *J. Am. Chem. Soc.* **2004**, *126*, 13033–13043.
- (9) All entries that employ AgOTf were corrected according to reference 5d. The raw H/D exchange data for all catalytic transformations with trifluoroacetic acid- $d_1$  were corrected by subtraction of the percent deuterium incorporation observed in the background reaction between trifluoroacetic acid- $d_1$  and  $C_6H_6$  in the presence of AgCl, which is formed in situ when AgOTf is added to a catalyst. Under the conditions for the catalytic reaction, there is not a significant amount of AgOTf present.
- (10) The H/D exchange reaction is clearly complicated, involving many steps and many transition states; thus, our utilization of isotope effects here is just to show that the effect of isotopic substitution is different in the different solvents for the H/D exchange reactions. We do not presume to know the origin of these isotope effects, that is, whether they are kinetic isotope effects or equilibrium isotope effects.
- (11) The concentration of benzene in methanol may affect the dielectric constant. However, curvature in the TOF vs [benzene] commences at concentrations much less than 1 M. At concentrations such as these, the dielectric constant of the solvent is not expected to change significantly. Further, the trend in saturation is seen not only for catalyst **4** but also for several other catalysts used in this study.
- (12) The elementary steps proposed for C–H activation in methanol are standard (for a discussion on mechanisms for C–H functionalization, see: Hartwig, J. F. *Organotransition Metal Chemistry: From Bonding to Catalysis*; University Science Books: Mill Valley, CA, 2010; pp 825–826), that is, an organometallic species activates benzene to form an Ir–Ph complex. This complex then reacts with the deuterium source to generate the deuterated product. We do not speculate on the exact nature of the organometallic species at this time, neither do we speculate about the nature of the C–H activation mechanism because we do not have any evidence to support these claims and such a study is beyond the scope of this manuscript.
- (13) After 600 min, the catalyst appears to be deactivated. However, thermal stability studies of the catalyst in this solvent did not reveal any evidence of a new Ir species, neither was there any evidence of iridium black.
- (14) To derive,  $d[\text{Ph-D}]/dt = k_1[\text{Ph-H}][\text{D}^+]$ . Since  $[\text{M}(\text{OTFA})] = [\text{D}^+]$ , then  $K_D = [\text{D}^+]^2/[\text{M}]$ .  $K_D[\text{M}]^{1/2} = [\text{D}^+]$ .  $d[\text{Ph-D}]/dt = k_1K_D[\text{Ph-H}][\text{M}]^{1/2}$ .
- (15) Reactions were performed in acetic acid- $d_4$ , as well; however, no H/D exchange was observed with *t*-butyl benzene in this solvent.
- (16) (a) Colby, D. A.; Bergman, R. G.; Ellman, J. A. *Chem. Rev.* **2010**, *110*, 624–655. (b) Boutadla, Y.; Davies, D. L.; Jones, R. C.; Singh, K. *Chem.—Eur. J.* **2011**, *17*, 3438–3448. (c) Alberico, D.; Scott, M. E.; Lautens, M. *Chem. Rev.* **2007**, *107*, 174–238. (d) Guimond, N.; Gorelsky, S. I.; Fagnou, K. *J. Am. Chem. Soc.* **2011**, *133*, 6449–6457. (e) Maleckis, A.; Kampf, J. W.; Sanford, M. S. *J. Am. Chem. Soc.* **2013**, *135*, 6618–6625. (f) Boutadla, Y.; Al-Duaij, O.; Davies, D. L.; Griffith, G. A.; Singh, K. *Organometallics* **2009**, *28*, 433–440. (g) Davies, D. L.; Macgregor, S. A.; Poblador-Bahamonde, A. I. *Dalton Trans.* **2010**, *39*, 10520–10527.
- (17) Boutadla, Y.; Davies, D. L.; Macgregor, S. A.; Poblador-Bahamonde, A. I. *Dalton Trans.* **2009**, *38*, 5887–5893.
- (18) Isobe, K.; Bailey, P. M.; Maitlis, P. M. *J. Chem. Soc., Dalton Trans.* **1981**, 2003–2008.
- (19) To test for heterogeneity, a mercury drop experiment was performed in this solvent. No evidence for catalyst inhibition was observed.
- (20) (a) Hettler, D. G. H.; Reek, J. N. H. *Chem. Commun.* **2011**, *47*, 2712–2714. (b) Xiao, X.-Q.; Jin, G.-X. *J. Organomet. Chem.* **2008**, *693*, 3363–3368. (c) Cayemittes, S.; Poth, T.; Fernandez, M. J.; Lye, P. G.; Becker, M.; Elias, H.; Merbach, A. E. *Inorg. Chem.* **1999**, *38*, 4309–4316. (d) Ogo, S.; Makihara, N.; Watanabe, Y. *Organometallics* **1999**, *18*, 5470–5474.